JOURNAL OF COLLOID AND INTERFACE SCIENCE 169, 168–176 (1995)

On the Physical Adsorption of Vapors by Microporous Carbons

R. H. BRADLEY*,[1] AND B. RAND†

*Institute of Surface Science and Technology, University of Technology, Loughborough, Leicestershire, LE11 3TF United Kingdom; and †Division of Ceramics, School of Materials, University of Leeds, Leeds, LS2 9JT United Kingdom

Received February 4, 1994; accepted May 25, 1994

The physical adsorption of nonpolar and polar vapors by active carbons is discussed in relation to pore structure and pore wall chemistry. For nonpolar vapors the Dubinin–Radushkevich equation is used to derive micropore volumes (W_0), average adsorption energies (E_0), and micropore widths (L) for a number of systems. These parameters are used to interpret the adsorption behavior of nitrogen which, because it is a relatively small molecule, is frequently used at 77 K to probe porosity and surface area. Results are presented for three carbons from differing precursors, namely, coal, coconut shells, and polyvinylidene chloride (PVDC) to illustrate the applicability of the technique. For the latter carbon increases in micropore size, induced by activation in carbon dioxide, and reductions in accessible pore volume caused by heat treatment in argon are also characterized and related to structural changes. The approach is then extended to the adsorption of larger hydrocarbon vapors, where the resulting W_0 values may require correction for molecular packing effects which occur in the lower relative pressure regions of the isotherms, i.e., during the filling of ultramicropores. These packing effects are shown to limit the use of the Polanyi characteristic curve for correlating isotherm data for several vapors, of differing molecular sizes, by one adsorbent. Data for the adsorption of water, which is a strongly polar liquid, have been interpreted using the Dubinin–Serpinsky equation. In particular the characteristic water adsorption value [a_0] of that equation is used to follow the changes in adsorption character of the PVDC carbons. Results indicate that activation in carbon dioxide increases the polarity of the carbon structure leading to a corresponding increase in the heat of immersion (ΔH_i). Heat treatment in argon appears to thermally desorb polar species leading to lower values of a_0 and (ΔH_i).

Key Words: activated carbons; adsorption; micropore structure; surface chemistry; Dubinin theory.

1. INTRODUCTION

1.1. Adsorption Theory

The physical adsorption of nonpolar vapors occurs by induced dipole-induced dipole (dispersion) interactions of the type described by London (1, 2). For active carbons which contain a distribution of pore sizes, these forces determine monolayer and multilayer adsorption at high relative pressures in wider pores (>2 nm.) and onto open surfaces. However, the dominant feature of the adsorption process is the volume filling of the smaller micropores as described by Dubinin and his co-workers (3, 4). This latter process occurs at lower relative pressures than monolayer and multilayer adsorption because of the enhanced dispersion interaction resulting from the overlap of potential energy wells which results as a consequence of the close proximity of the pore walls as shown in Fig. 1 (5). The process is effectively determined by the micropore structure of the carbon and in particular the relative sizes of the adsorptive molecules to the average slit width of the micropores. The maximum effect occurs when the adsorptive is of similar dimension to the average width or radius of the micropore as shown in Fig. 2. At the lowest adsorption pressures, i.e., during the filling of ultramicropores (<1 nm width or radius), the process may be complicated by molecular sifting, whereby molecules are physically excluded from certain volumes of microporosity because of their large size. The process known as activated diffusion, whereby adsorptive molecules do not possess sufficient kinetic energy to overcome the free energy barrier to pore entry, may also influence the adsorption process in this region of the isotherm.

The adsorption of nonpolar vapors in micropores gives rise to type 1 (BDDT (6)) isotherms which can be interpreted using the Dubinin–Radushkevich equation (7)

$$W = W_0 \exp[-(A/\beta E_0)]^2 \qquad [1]$$

in conjunction with the corresponding characteristic curve of the Polanyi Potential theory (8)

$$W = NV_m = f(A/\beta). \qquad [2]$$

By convention, W is the volume of adsorbate within the pore structure at relative pressure p/p^0 (p being the equilibrium and p^0 the saturation vapor pressures at the adsorption temperature T). N is the molar adsorption value per gram of adsorbent and V_m is the molar volume of the liquid adsorbate. W_0 is the micropore volume of the adsorbent. The

[1] To whom correspondence should be addressed.

0021-9797/95 $6.00

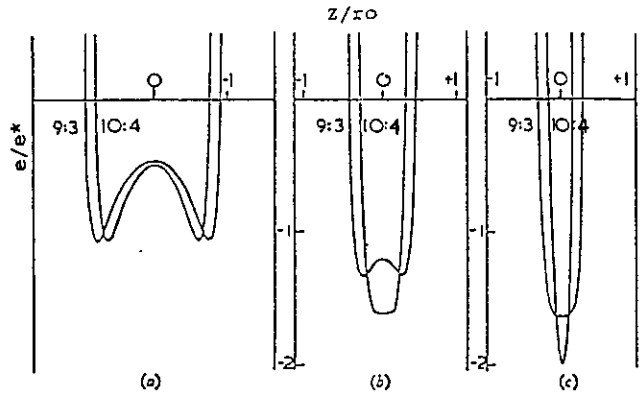

FIG. 1. Increasing enhanced potential in slit-shaped pores as the ratio d/r^0 approaches unity. The potential e is shown compared to the potential associated with an open surface e^*. Redrawn from Ref. (5).

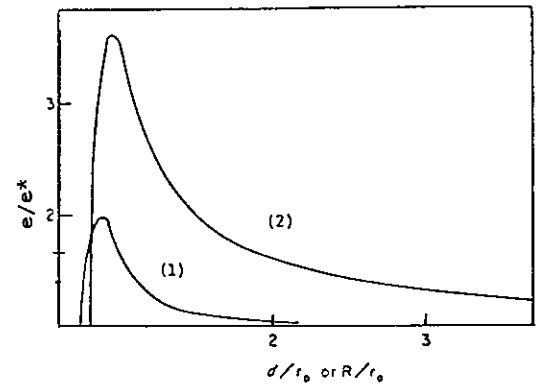

FIG. 2. Enhanced interaction in (1) slit-shaped pores of diameter (d) and (2) cylindrical pores of radius (R) from Ref. (5).

term adsorption potential (A) was used by *Polanyi* and defined as $A = RT \ln p^0/p$ (R being the molar gas constant). Dubinin used the phrase *differential molar work of adsorption* with the bulk liquid at the adsorption temperature as the reference state. In either case $A = -\Delta G$ with ΔG being the differential free energy of adsorption. The affinity coefficient, β, describes the adsorbability of the adsorptive and is calculated by comparing physical parameters, e.g., molar volume, against a suitable reference adsorbate, traditionally benzene (9). Consequently, a plot of W against A/β should result in the coincidence of a family of characteristic curves for the adsorption of a range of vapors by one adsorbent. The characteristic adsorption energy, E_0, is a function of the micropore size distribution of the adsorbent.

Equation [1] has been shown to linearize type 1 adsorption isotherm data over very wide ranges of relative pressure, often several orders of magnitude of p/p^0, and it has found widespread use for deriving micropore volumes in characterization and comparative studies of active carbons. Deviations from linearity are often observed in plots of the equation. These may occur at both extremes of pressure and have been classified and discussed in detail by Marsh and Rand (10). Figure 3 shows typical rectilinear plots of Eq. [1] with three common types of nonlinear deviations. Type A deviations at low relative pressures (high values of $\log^2 p^0/p$ and therefore $A = RT \ln p^0/p$) occur in the region of the adsorption isotherm where the narrowest pores are being filled. They are often observed for molecular sieve materials and are therefore frequently attributed to activated diffusion. They have also, however, been reported for wider pore materials, e.g., carbons activated to a high degree of burn off. Here, explanation by kinetic effects is less satisfactory unless activation has occurred nonuniformally (i.e., in a kinetically controlled rather than a chemically controlled Arhenius regime) and a proportion of narrow pores are retained giving rise to a relatively wide distribution of adsorption potential. Type B curves appear to be particularly characteristic of CO_2 adsorption. Type C behavior, at high pressures, results from adsorption in pores wider than those associated with micropore filling and are therefore a consequence of a bimodal distribution of A with W.

The characteristic adsorption energy E_0 is a mean value for the micropore size range being filled, as defined by the linear region of the D–R plot. It has been shown that for slit-shaped and cylindrical model micropores (5) adsorption potential is inversely related to either the half-width or radius of these respective pore types. Therefore, E_0 is expected to vary as a direct result of structural changes such as pore widening due to activation, or pore narrowing as a result of heat treatment or impregnation of the pore network with active species. On the basis of small angle X-ray scattering (SAXS) data (11, 12) analyzed using the Guinnier equation (13), Dubinin and Stoeckli (14) have proposed that for a pure carbon the following inverse relation between E_0 and R_g, the average radius of gyration of the pores being filled

$$E_0 R_g = 14.8 + 0.6 \ (\text{nm} \cdot \text{kJ} \cdot \text{mol}^{-1}). \qquad [3]$$

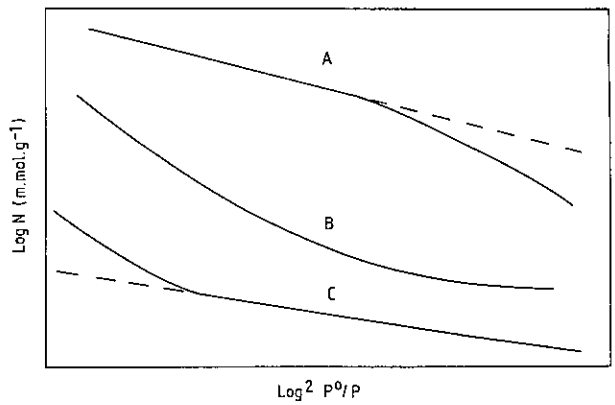

FIG. 3. Deviations from linearity of Dubinin–Radushkevich plots from Ref. (10).

However, this equation may only be appropriate for a limited range of micropore sizes and it has been suggested by McEnaney that the expression which may be more generally applicable (15) is

$$W_m = 4.691 \exp(-0.0666\, E_0), \quad [4]$$

where W_m is the pore width accessible to molecular probes. In this instance the Guinnier parameter Rg is given by

$$Rg = 0.055 + 0.55\, W_m\,(\text{nm}). \quad [5]$$

Generally, the average width of the pores being filled (L/nm) can be obtained from the following relation [6], where K takes a value of 16.5–18 $kJ \cdot nm \cdot mol^{-1}$ (16). Several other similar expressions have also been proposed.

$$L = K/E_0 \quad [6]$$

The adsorption of polar vapors, such as water, by active carbons results in a type 5 isotherm. In the generally accepted model for the adsorption of such species, adsorption in the initial region of this isotherm occurs by the hydrogen bonding of water molecules onto specific adsorption sites. For pure carbons these are effectively oxygen molecules chemisorbed at the edges of the carbon layers (17–19) but in less pure materials it is likely that other heteroatoms, such as nitrogen, will also constitute polar sites. Using this approach, the shape of the initial region of the adsorption isotherm is determined by the polarity, i.e., the surface chemistry, of the accessible surfaces (basal plane or edge area) of the carbon structure, while the remainder of the isotherm describes the bulk filling of the porosity of the carbon. Kiselev has shown that the steep regions of type 3 isotherms, obtained for water adsorption by carbon blacks, can be displaced to higher values of relative pressure by the thermal desorption of chemisorbed oxygen (19). Stoeckli has demonstrated similar behavior for type 5 isotherms from microporous carbons (20). In each case the decrease in surface polarity leads to an increase in the hydrophobicity of the carbon structure. Dubinin and Serpinsky (17) have used to characterize the number of primary adsorption sites from static water isotherms for active carbons the equation

$$a = a_0 ch/(1 - ch), \quad [7]$$

where the term (a) is the amount of water adsorbed (usually expressed as $m \cdot mol \cdot g^{-1}$) at any given value of relative pressure $h = p/p^0$, (a_0) is the specific amount of water adsorbed, calculated from Eq. [7], and is therefore characteristic of the surface polarity of the carbon structure, and c is the ratio between the overall rates of adsorption and desorption. Stoeckli *et al.* (21) have proposed that the enthalpy of immersion (ΔH_i) for pure carbons, i.e., where the carbon–water interaction is not complicated by the presence of mineral impurities, can be calculated by substituting a_0 from Eq. [7] into the relation

$$\Delta H_i/J \cdot g^{-1} = [-25.0/J \cdot mol^{-1}/(H_2O)]a_0 - [0.6/J \cdot mol^{-1}(H_2O)](a_s - a_0). \quad [8]$$

The term a_s is the limiting adsorption value at $p/p^0 \approx 1$. The term a_0 would be expected to increase with the oxidation of the carbon structure and decrease as oxides are thermally desorbed during heat treatment. The applicability of these approaches to the analysis of vapor adsorption data for several types of carbons is considered in Section 3 of this article where Eq. [1] is used to reveal structural characteristics and Eq. [7] is used to probe surface chemical information. In particular the characteristic parameters W_0, E_0, L, and a_0 are considered in relation to structural properties of carbons.

1.2. Structure of Active Carbons

Several models have been proposed for the structure of active carbons (22–24). The main features common to all are carbon layer planes, which show varying degrees of 2D and 3D order, and the spaces in between these layers which constitute porosity; this is represented schematically in Fig. 4. The interlayer spaces in the most ordered regions, where these materials are most *graphite-like* but still highly disordered, are termed *micropores.* These apertures are commensurate in size with many gaseous species (<2 nm), and in them adsorption occurs by the energetically enhanced process known as primary micropore volume filling. More disordered regions contain larger mesopores (size range 2 to 50 nm) and macropores (>50 nm). These size distinctions, which are the subject of a IUPAC classification document (25), result from the associated mechanisms of adsorption which operate within each range and they are therefore somewhat dependent upon the size of the adsorptive molecule used. In this vein micropores have been divided into two subgroups: *ultramicropores,* which fill by the *primary,* enhanced potential process already discussed, and *supermicropores,* with which is associated a *secondary,* cooperative mechanism of micropore filling (26).

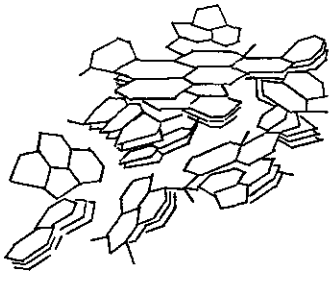

FIG. 4. Structure for disordered graphene layer model of microporous carbon.

The process of activation causes changes in carbon structure which lead to modification of the open porosity. The process may be physical or chemical. Physical activation (gasification) is a process of oxidation, usually carried out using steam or carbon dioxide, whereby carbon is removed from the structure as gaseous oxide (27). Chemical activation is particularly applicable to wood-based carbon and is achieved by mixing a suitable activating agent, such as zinc chloride or phosphoric acid, with the precursor material before carbonization is started (28). These processes lead to a shift in the pore size distribution of the carbon to higher average dimensions. This would be expected to increases the adsorptive capacity of a given carbon and may also lead to improved adsorption for certain bulky species by reducing molecular sifting. A schematic representation of the effects of activation upon the Dubinin–Radushkevich plot, the Polanyi characteristic curve a corresponding monomodal distribution of A with W, are shown in Fig. 5 for a carbon giving a type 1 isotherm. The overall behavior is characterized by a shift, to higher adsorption values of the isotherm, accompanied by a rounding of the knee. This leads to an increased overall adsorption volume, as reflected by W_0 for the linear D–R plot, but may also lead to some loss of low pressure adsorption if activation leads to the widening of ultramicropores which fill by the energy-enhanced mechanism. This gives an increase in slope of the D–R plot, which consequently then intercepts the pressure axis at a lower value of $\log^2 p^0/p$ and which is also characterized by a lower E_0 value and wider average pore width (L). The corresponding characteristic curve is shifted to lower values of A as is the distribution of A with W. Continued activation would lead to type C, positive deviation, in the D–R plot indicating a bimodal distribution of A with W.

Activation can also lead to an increase in the noncarbon content of the structure, for example, chemisorbed oxygen or other heteroatoms residual from impregnation treatments, these may act as sites which are capable of specific interactions with polar adsorptives. Conversely, heat treating carbons in an inert environment effectively anneals the structure and leads to pore narrowing; this is also accompanied by the removal of chemisorbed oxygen functionalities and consequently a decrease in surface polarity.

The results presented in this paper show clearly that the approach described in Section 1.1. can be used to obtain a detailed characterization of the adsorptive properties of active carbons in relation to their precursor and treatment history and the resulting structure and chemistry as described above.

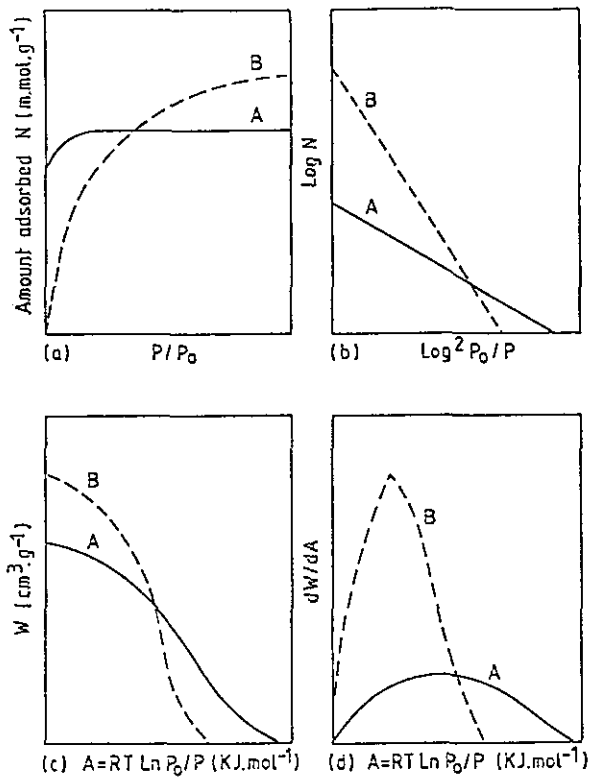

FIG. 5. Adsorption data for unactivated (A) and activated (B) carbons shown as (a) a normal isotherm plot, note the greater curvature in the knee region for the activated material B. (b) Dubinin–Radushkevich plot from Eq. [1] showing change of slope after activation. (c) Polanyi characteristic curve of Eq. [2]. (d) The distribution of adsorption potential $A = RT \ln p^0/p$ with W skewed to lower values after activation.

2. EXPERIMENTAL

Isotherm data have been determined using a static gravimetric apparatus using calibrated silica springs and CI microbalances. Carbon samples were outgassed at 523 K to constant weight and a residual pressure of 10^{-5} Torr. Equilibrium pressures were measured using a Baratron 0.01–100 Torr absolute transducer and a C.E.C. 0–760 Torr transducer. Kinetic plots of weight uptake with time were recorded to identify equilibrium weights. Adsorption temperatures were maintained using either liquid nitrogen (77 K) or a water ice slurry (273 K). Nitrogen and Freon 113 were supplied by BOC and introduced to the system after vacuum distillation. Physical details of these adsorbates are given in Table 1, values of β, used to produce the data shown in Fig. 7, have been calculated using molar volume data.

BPL, coal based, and SC11, nutshell, carbons were provided by Chemviron. Polyvinylidene chloride carbons were all produced from a single batch of commercial PVDC supplied by Dow Chemicals Ltd. Carbonization was carried out by heating in a horizontal tube furnace for 2.5 h at 1123 K in an atmosphere of dry oxygen-free nitrogen followed by cooling in the same atmosphere. These conditions cause dechlorination and/or dehydrochlorination of the PVDC (29) leading to an essentially pure carbon of the type extensively studied in the past (30, 31).

Samples of this S850 carbon were activated or heat treated, again in a tube furnace. Activation was carried out by flushing

TABLE 1
Physical Characteristics of Adsorptives

	Molecular weight	Saturation pressure (p^0) Torr at T_{ads}	Liquid density at T_{ads} (g cm^{-3})	Molar volume V_m (cm^3 mol^{-1})	Shifting factor β	T_{ads} (K)
Nitrogen	28.00	760.00	0.808	34.65	0.35	77
Methanol	32.03	93.28	0.79	40.81	0.45	293
Ethanol	46.07	43.90	0.79	53.32	0.64	293
Propan-2-ol	60.10	32.40	0.78	76.58	0.83	293
Butan-1-ol	74.12	4.30	0.81	91.51	1.01	293
Freon 113	187.38	385.5	1.62	115.56	1.19	273
Water	18.00	17.53	1.00	18.00	0.22	293

weighed samples of carbon in nitrogen for 15 min followed by an estimated burn off at 1173 K in a CO_2 flow of 20 cm^3 min^{-1}. Samples were cooled in N_2. Treatment in this way for 12 and 24 h gave 30% (S850-30%) and 65% (S850-65%) burn-off carbons. Heat treatments were carried out by purging samples of the S850 carbon in dry argon for 15 minutes after which time, with the argon still flowing, the sample was brought to the required HTT and held there for 10 minutes followed by cooling in argon. Samples treated in this way are prefixed S850 followed by the HTT in kelvins i.e., S850-1273, S850-1473 and S850-1673.

3. RESULTS AND DISCUSSION

3.1. Characterization of Pore Structures

Table 2 contains total pore volumes (V at $p/p^0 \approx 0.98$) for the two commercial carbons obtained by the adsorption of a range of vapors. The data give an excellent example of Gurvitsch behavior (32), i.e., that correction of the limiting molar adsorption value for any given adsorptive, using its corresponding liquid density at the adsorption temperature, should result in effectively the same characteristic volume for one solid. However, because active carbons commonly contain a wide distribution of pore sizes characterized by a bimodal distribution of adsorption potentials, a more refined approach is required to allow a more rigorous analysis. Equation [1] is frequently applied to separate the higher adsorption potential process of micropore filling from lower energy adsorption in wider pores and onto open surfaces which occurs at higher pressures. This allows determination of a micropore volume for the adsorbent, the error of precision usually being <10%. This approach can be used to determine specific adsorption characteristics for individual carbons as shown in Table 3, where the parameters from Eq. [1] are compared for the two commercial carbons and the PVDC carbon. The coal- and nutshell-based materials are shown to contain similar volumes of porosity but the pores in the nutshell-based material are narrower, when defined by the dimension parameter L, than those of the coal-based carbon. The pores in PVDC are all narrow (<0.7 nm), there is less difference between V and W_0, and therefore proportionately less adsorption in the low A mode.

A consequence of Eq. [2] is that adsorption data for a specific adsorptive adsorbed at varying temperatures onto a single adsorbate should coincide if corrected using the molar liquid volumes of the adsorbate at the relevant temperatures. This temperature invariance of the characteristic curve was first illustrated by Dubinin (33) and an example is given in Fig. 6 for carbon dioxide adsorption by a nutshell carbon from the data of Amberg *et al.* (34). It follows that data for the adsorption of different vapors onto a single adsorbent corrected for molecular volume should also coincide. A plot of Eq. [2] (W against A/β) for the BPL system, Fig. 7, shows

TABLE 2
Saturation Volumes (V) and Micropore Volumes (W_0 from Vapor Adsorption onto Coal-Based (BPL) and Nutshell-Based (SCII) Carbons

	BPL		SC11	
	W_0	V	W_0	V
Nitrogen	0.43	0.50	0.40	0.47
Methanol	0.42	0.48	0.44	0.46
Ethanol	0.43	0.48	0.44	0.46
Propanol	0.43	0.48	0.45	0.48
Butanol	0.43	0.46	0.43	0.45

TABLE 3
Comparison of Characteristic Parameters from Eq. [1] for Three Active Carbons

	Nitrogen 77 K			
	V (cm^3 g^{-1})	W_0 (cm^3 g^{-1})	E_0 (kJ mol^{-1})	L (nm)
BPL Coal-based	0.50	0.43	19.1	0.99
SC11 Nutshell-based	0.47	0.40	23.5	0.73
S850 PVDC-based	0.41	0.38	25.3	0.68

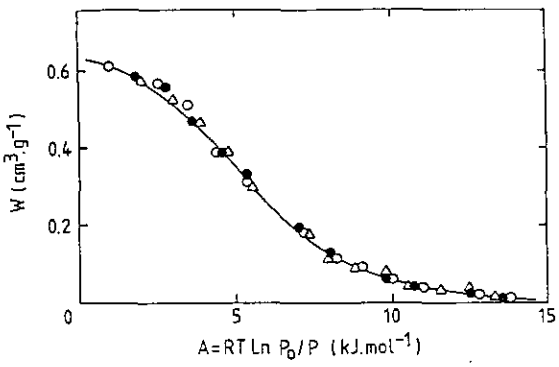

FIG. 6. Temperature invariance of characteristic curves demonstrated for carbon dioxide adsorption at 182, 188, and 196 K by a nutshell carbon. Data from Ref. (34).

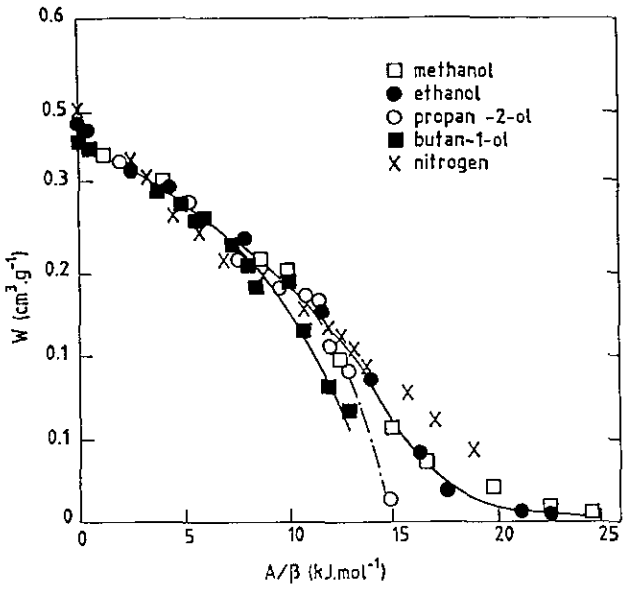

FIG. 7. Characteristic curves for adsorption by BPL coal-based carbon plotted using β values calculated from molar volume data.

that data for a range of vapors only coincide over the higher pressure ($A < \approx 10$ kJ mol^{-1}) region of the measured pressure range and that in the low pressure (high A) regions the isotherms are differentiated according to the relative molecular sizes of the adsorptives. While this indicates that each vapor sees a different distribution of micropore sizes and corresponding adsorption potentials, this is not evident in the W_0 values, shown in Table 3. These deviations are thought to be due to molecular packing restrictions, within ultramicropores, at the lowest adsorption pressures and consequently may mean that the assumed liquid density for the adsorbed phase is incorrect in that region of the isotherm (35) and that a density value which changes differentially with micropore filling may be more appropriate. The thermodynamic state of the adsorbed phase within micropores has recently been considered further by Dubinin (36), in terms of compressibility for benzene adsorption, and Aukett *et al.* (37) in terms of density correction for adsorbed nitrogen. Both approaches lead to increased estimates of the higher adsorption mode volume (by a factor of approximately 1.15) than those obtained from Eq. [1].

The use of active carbons for the selective adsorption of gaseous molecules is well established (38) and in this respect a significant feature of these materials is that their pore size distributions can be modified using the processes of activation or heat treatment. The activation of carbons generally leads to displacement of the isotherm to higher adsorption values as a consequence of increased pore dimension and capacity. This process is usually accompanied by a rounding of the isotherm knee as illustrated in Fig. 5a. This behavior is clearly demonstrated for activated PVDC-based materials in Fig. 8. It has been shown that over a wide range of activation (burn off 5 to 90%) the pore volumes actually pass through a maximum value declining thereafter due to excessive pore widening and loss of carbon. Heat treatments at increasing temperatures cause progressive displacement of the isotherms to lower adsorption values which correspond to loss of open porosity due to the closure of pore apertures and/or reductions in inter carbon-layer spacing (39). Characterization of a series of carbons which have been modified using these methods is illustrated in Table 4 which shows the effects of both processes on the resulting adsorption behavior for nitrogen and the much larger trichloro-, trifluoroethane (Freon 113) molecule. The isotherms have been analyzed using the Dubinin–Radushkevich approach, and Fig. 9 shows the data for the activated materials plotted in the form of Eq. [1].

Very little increase in W_0 or V is evident between 30 and 65% burn off, but an increases in slope of the plot for the

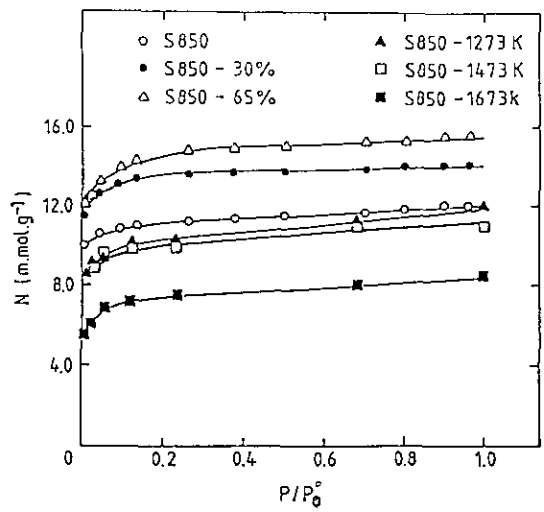

FIG. 8. Nitrogen adsorption isotherms for untreated (S850) activated (30 and 65% burn off) and heat-treated (1273, 1473, and 1673 K) PVDC carbons.

S850-65% is indicative of pore widening. Activation leads to an increase in N_2 adsorption by 20–30%. Increases in adsorption with burn off are frequently more marked for large molecules as shown by the Freon 113 data which show a factor of 2 increase suggesting that steric factors are suppressing the adsorption of the larger vapor in the case of unactivated S850 carbon.

Heat treatment leads to the marked exclusion of Freon 113 from volumes of porosity open to N_2. Figure 8 shows that the amounts of N_2 adsorbed by the S850-1273 and S850-1473 samples are very similar. However, as shown in the table, the Freon values differ markedly, indicating that the pore entrances of the 1473 material are narrower than those of the 1273 carbon.

Generally, increasing the heat treatment temperature causes a progressive decrease in both W_0 and V consistent with the accepted mechanism of pore closure and reductions in inter-layer spacings which occur during the HT process (39). N_2 volumes do not change greatly for the 1273 and 1473 K materials but are markedly lower for the 1673 K carbon. Previous studies have indicated activated diffusion for argon adsorbed at 77 K by cellulose-based carbons heat treated at temperatures of 1470 K; this led to an increase in equilibrium time from 3 to 168 h (23). No such effects were detectable for the nitrogen and Freon adsorption onto the PVDC carbons. The low uptakes for Freon are thought to be due to physical exclusion.

The E_0 values obtained for the activated carbons from the N_2 data are commensurate with values obtained by other schools for the filling of ultramicropores (40). The N_2 values decrease with burn off as the pores become wider, and they also agree closely with figures obtained by McEnaney (41) for the adsorption of Ar at 77 K onto PVDC carbons of similar burn offs. Deriving these parameters from the Freon 113 data indicates that only the wider pores are being probed by this large molecular; however, for the 65% burn off carbon, where steric effects are minimized, the values obtained for E_0 and L are very close to the N_2 values.

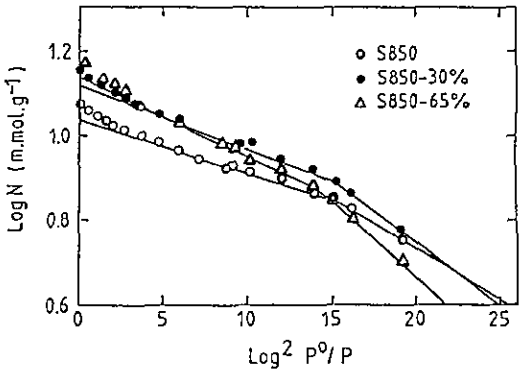

FIG. 9. Dubinin–Radushkevich plots for nitrogen adsorption at 77 K by S850 and activated PVDC carbons.

When nitrogen is the adsorbate on the HT carbons an increase in E_0 is observed for the 1273 K material as new ultramicropores are opened and developed. Both the 1273 and the 1473 K carbons give N_2 W_0 values which are similar to the parent S850, but in the case of the 1473 K an increase in slope of the plot leads to a lower E_0 value, indicative of closure of narrow pores. This effect becomes more marked for the 1673 K carbon where a significant reduction in W_0 is also observed.

3.2. *Surface Polarity and Water Adsorption*

Type 5 isotherms are observed for all five of the carbons studied; examples are given in Fig. 10. Table 5 shows that the saturation volumes for water adsorption by these carbons (a_s) show similar trends to those already discussed for nitrogen and Freon 113 saturation (V) by these materials in that the water volumes recorded for the activated carbons increase with burn off, compared to the S850 parent material, while increasing the heat treatment temperature leads to a decrease in the total volumes of water adsorbed.

As is normally observed, the water volumes are lower than both the nitrogen saturation volumes and the Dubinin–Ra-

TABLE 4
Characteristic Parameters for Untreated, Activated, and Heat-Treated PVDC-Based Carbons from Nitrogen Adsorption at 77 K and Tri Chloro, Trifluoro ethone (freon 113) at 273 K

	Nitrogen 77 K				1,1,2-trichloro-1,2,2-trifluoroethane			
	V ($cm^3\ g^{-1}$)	W_0 ($cm^3\ g^{-1}$)	E_0 ((K)mcl^{-1})	L (nm)	V ($cm^3\ g^{-1}$)	W_0 ($cm^3\ g^{-1}$)	E_0 ((K)mcl^{-1})	L (nm)
S850-65%	0.54	0.48	20.2	0.85	0.43	0.42	19.8	0.87
S850-30%	0.49	0.46	22.7	0.76	0.40	0.38	19.4	0.89
S850	0.41	0.38	25.3	0.68	0.22	0.18	15.5	1.11
S850-1273	0.37	0.35	26.5	0.65	0.06	0.06	15.8	1.09
S850-1473	0.38	0.33	22.7	0.76	0.02	0.01	9.8	1.76
S850-1673	0.29	0.24	20.5	0.84	0.003	0.003	5.5	3.14

dushkevich micropore volumes W_0 for each carbon. This has in the past been explained in terms of a lower density for water in the adsorbed phase compared to that of the normal bulk liquid (42). The ratios of the volumes a_s/V show that the water values are 50–80% of those obtained by nitrogen adsorption. Further, these ratios increase with burn off or decrease with increasing heat treatment temperature, which suggests that the degree of pore filling achieved at $h \approx 1$ is influenced by the polarity, and therefore the wettability, of the carbons pore walls. For a heat-treated carbon, where the internal pore walls have a decreased polarity, the ease with which an adsorbed water film can form and spread is less than that which might be expected for an oxidized carbon. Thus, a decrease in polarity of a carbon structure may give rise to volumes of porosity which do not completely fill with water. These are most likely to be the micropores which, because they occur in between the carbon layers, have pore walls with basal-plane character which are of low polarity.

Application of the Dubinin–Serpinsky (Eq. [7]) to the water isotherm data allows derivation of the parameter a_0 for the carbons studied. These values have then been used to calculate heats of immersion (ΔH_i) from Eq. [8]. Values for both of these parameters (Table 5) show a decrease from the value obtained for the S850-65% burn off material to that of the S850-1673 K heat-treated carbon which is consistent with a decrease in surface polarity due to the progressive desorption of chemisorbed oxygen with increasing HTT and the increase in polarity caused by oxidation of the carbon structure with burn off, i.e., as more basal-plane edge area is exposed.

It has been argued that the basis of Eq. [7] is that adsorption occurs by hydrogen bonding between water molecules and specific primary adsorption sites (surface oxides). Adsorbed water molecules then constitute secondary adsorption sites which are further available for hydrogen bonding. Thus, the mechanism involves the formation of molecular clusters, initially centered at specific sites, which coalesce as adsorption proceeds and eventually lead to bulk pore filling as (a) approaches the value of (a_s). A direct relationship should therefore exist between a_0 and the absolute concentration of oxide species contained by a given pure carbon and the best fit to Eq. [1] should occur in the range over which the isotherm (type 3 or 5) curves away from the pressure axis, i.e., where adsorption is determined by the primary sites. This has been shown not to be the case for these systems and consequently the physical meaning of the parameter a_0 and its ability to describe the absolute concentration of oxides present appears to be uncertain (43).

TABLE 5
Characteristic Parameters from Water Adsorption

	a_s (m·mcl·g^{-1})	a_s/V	a_0 (m·mcl·g^{-1})	ΔH_i (J·g^{-1})
Activated S850-65%	0.41	0.76	2.99	−86.6
Activated S850-30%	0.36	0.73	1.94	−59.6
Untreated S850 char	0.26	0.63	2.23	−55.7
Heat treated S850-1273	0.18	0.49	1.41	−40.3
Heat treated S850-1473	0.24	0.63	0.37	−16.8
Heat treated S850-1673	0.15	0.52	0.15	−11.8

Note. Saturation water adsorption volumes (a_s), water/nitrogen ratios (a_s/V), Dubinin–Serpinsky characteristic water adsorption values (a_0), heat of immersion from Eq. [8] (ΔH_i).

4. CONCLUSIONS

The adsorption of nonpolar vapors by active carbons is determined by nonspecific dispersion interactions. Adsorption within micropores, at low pressures, is characterized by an enhanced adsorption potential due to the close proximity of the pore walls and is distinct from adsorption in mesopores and macropores which fill at higher relative pressures. This gives rise to a bimodal distribution of adsorption potentials but with most of the adsorption occurring at low pressures, i.e., in the high energy mode, which results in isotherm data of type-1 character. Analysis of this data, using the Dubinin approach, allows calculation of a micropore volume for the high A mode and also leads to a dimensional parameter for the average pore being filled. These parameters can be used to follow changes caused by structural modification of the carbon.

In contrast, the adsorption of polar vapors, such as water, occurs initially at specific adsorption sites by hydrogen bonding. This leads to a nucleation-type process whereby individual clusters of adsorbed molecules coalesce to fill the pore structure. The adsorption sites are heteroatoms such as

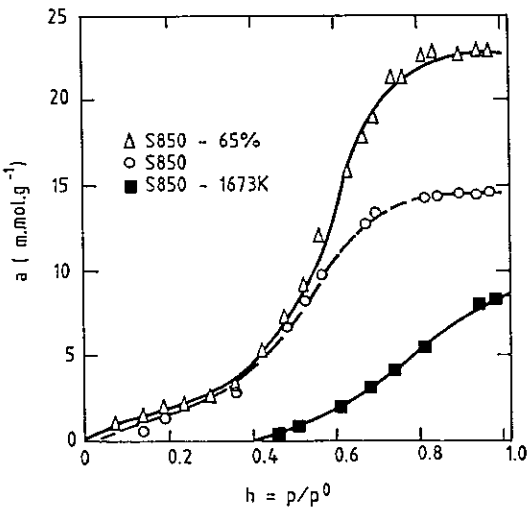

FIG. 10. Type 5 isotherms for adsorption of water vapor by PVDC carbons at 293 K.

oxygen or other chemisorbed species, residual from the carbons precursor or specific chemical treatment(s). Consequently, analysis of the initial region of water adsorption isotherms can give qualitative information about the concentration of these heteroatoms and the resulting polarity of the structure. Water adsorption volumes are difficult to interpret in terms of pore structure but, when compared to pore volumes from nonpolar vapors, they may give additional information about structural polarity.

REFERENCES

1. London, F., *Z. Physik.* **63,** 245 (1930).
2. London, F., *Z. Physik. Chem.* **11,** 222 (1930).
3. Dubinin, M. M., and Zavarina, E. D., *Zhur. Fiz. Khim.* **23,** 1129 (1949).
4. Dubinin, M. M., *Q. Rev. Chem. Soc.* **9,** 101 (1955).
5. Everett, D. H., and Powl, J. C., *J. Chem. Soc., Faraday Trans. 1* **72,** 619 (1976).
6. Brunauer, S., Deming, L. S., Deming, W. S., and Teller, E., *J. Am. Chem. Soc.* **62,** 1723 (1940).
7. Dubinin, M. M., and Radushkevich, L. V., *Proc. Acad. Sci. USSR* **55,** 331 (1947).
8. Polanyi, M., *Verh. Dtsch. Phys. Ges.* **16,** 1012 (1914).
9. Dubinin, M. M., and Timofeyev, D. P., *DPCR. Acad. Sci. USSR* **54,** 701 (1946).
10. Marsh, H., and Rand. B., "Proceedings, 3rd Conference on Industrial Carbon and Graphite," Soc. Chem. Ind., London, 1970.
11. Dubinin, M. M., and Plavnik, G. M., *Carbon* **2,** 261 (1964).
12. Dubinin, M. M., and Plavnik, G. M., *Carbon* **6,** 184 (1968).
13. Guinnier, A., and Fournet, G., *in* "Small Angle Scattering Of X-rays," Wiley, New York, 1955.
14. Dubinin, M. M., and Stoeckli, H. F., *J. Colloid Interface Sci.* **75,** 34 (1980).
15. McEnaney, B., *Carbon* **25,** 69 (1987).
16. Stoeckli, F., *Carbon* **28,** 1 (1990).
17. Dubinin, M. M., Zaverena, E. D., and Serpinsky, V. V., *J. Chem. Soc.* **2,** 1760 (1955).
18. Dubinin, M. M., *Carbon* **18,** 355 (1980).
19. Kiselev, A. V., and Kovalera, N. V., *Izv. Akad. Nauk SSSR, Otd. Khim. Nauk* 955 (transl.) (1959).
20. Stoeckli, H. F., and Kraehenbuehl, F., *Carbon* **19**(5), 353 (1981).
21. Stoeckli, H. F., Kraehenbuehl, F., and Morel, D., *Carbon* **21**(6), 589 (1983).
22. Oberlin, A., Viley, M., and Combaz, A., *Carbon* **18,** 347 (1980).
23. Masters, K. J., and McEnaney, B., *Carbon* **22**(6), 595 (1984).
24. Bansal, R. C., Donnet, J. B., and Stoeckli, F., *in* "Active Carbon," p. 120. Dekker, New York, 1988.
25. "IUPAC Manual of Symbols and Terminology," Appendix 2, Pt. 1, Colloid and Surface Chemistry, Pure and Applied Chem., Vol. 31, p. 578, 1972.
26. Gregg, S. J., and Sing, K. S. W., *in* "Adsorption, Surface Area and Porosity," 2nd ed., p. 266. Academic Press, London, 1982.
27. Ref. (24), p. 27.
28. Ref. (24), p. 8.
29. Edwards, F. G., "Encyclopedia of Polymer Science" (Mark, Gayland, and Bikales, Eds.), Vol. 14, p. 565. Interscience, New York, 1979.
30. Dacey, J. R., and Thomas, D. G., *Trans. Faraday Soc.* **50,** 740 (1954).
31. Culver, R. V., and Heath, N. S., *Trans. Faraday Soc.* **51,** 1569 (1955).
32. Gurvitsch, L., *J. Phys. Chem. Soc. Russ.* **47,** 805 (1915).
33. Dubinin, M. M., *in* "Chemistry and Physics of Carbon," Vol. 2, (P. L. Walker, Ed.), Dekker, New York, 1966.
34. Amberg, C. H., Everett, D., Ruiter, L. H., and Smith, F. W., *in* "2nd International Congress On Surface Activity," Vol. 2, p. 3. Butterworths, London, 1957.
35. Bradley, R. H., and Rand, B., *Carbon* **29,** 8 (1991).
36. Dubinin, M. M., Neimark, A. V., and Serpinsky, V. V., *Carbon* **31,** 7 1015 (1993).
37. Aukett, P. N., Quirke, N., Riddiford, S., and Tennison, S. R., *Carbon* **30**(6), 913 (1992).
38. Ref. (24), p. 335.
39. Masters, K. J., and McEnaney, B., *in* "The Characterisation of Porous Solids" (S. J. Gregg, K. S. W. Sing, and H. F. Stoeckli, Eds.), Soc. Chem. Ind., London, 1979.
40. Dubinin, M. M., and Stoeckli, F., *J. Colloid Interface Sci.* **75,** 34 (1980).
41. McEnaney, B., *Carbon* **25,** 69 (1987).
42. Ref. (26), p. 266.
43. Bradley, R. H., and Rand, B., *Carbon* **31,** 2 (1993).